Tension testing of additively manufactured specimens of 17-4 PH processed by Bound Metal Deposition

Tension testing of additively manufactured specimens of 17-4 PH processed by Bound Metal Deposition

F Bjørheim* and I M La Torraca Lopez

Department of Mechanical and Structural Engineering and Materials Science, University of Stavanger, Norway

*Corresponding author: fredrik.bjorheim@uis.no

Abstract. In contrast to the traditional ways of subtractive manufacturing, additive manufacturing (AM), also known as 3D printing, adapts computer-aided design to iteratively build the component or part layer by layer. The technology has recently gained a high momentum, both within academia, but also within the industrial sector. However, it is common that parts produced by AM will have more defects than parts produced by traditional methods. The objective of this paper is to investigate a new method of additive manufacturing, namely the bound metal deposition method (BMD). This method seemed promising from the perspective that the metal is not iteratively being melted, similar to such as welding. In fact, the part is first printed, then washed, for then to be sintered. Consequently, avoiding the complex thermal histories/cycles. It was found that the material will exhibit anisotropic behaviour, and have a mesh of crack like defects, related to the printing orientation.

1. Introduction

Additive manufacturing (AM), often called 3-D printing can be defined as the process that fabricates complex or customized solid free form parts using computer aided design (CAD). The process consists of iteratively adding layer by layer of materials, in contrast to conventional methods of subtractive manufacturing (e.g., cutting, drilling, grinding and machining) [1].

AM is changing both the way products are designed and manufactured, and has been used in many industries, such as automotive, aerospace, energy, oil and gas, health care, industrial and remanufacture industries, amongst others [2].

Some of the advantages worth mentioning regarding AM technology might be such as design freedom, the possibility of fabricating complicated geometries with complex internal structures, which are difficult if not impossible to build using traditional manufacturing techniques [3]. Furthermore, mass customization, as in producing a number of customized parts can be as cost-effective as mass production of identical parts. This from the perspective of the design freedom, that the manufacturing process is not dependent on such as molds and tooling [4]. Fast prototyping, the part or component can be produced directly from the computer aided design (CAD) software, with the addition of developing the printing pattern for the component. Consequently, reducing the need of many of the conventional processing steps and expensive tooling [5]. Another advantage worth mentioning is higher material efficiency, or waste minimization. This from the perspective that material is iteratively added in contrast to subtraction as per traditional methods [6]. In addition, parts can be manufactured on site by the method of AM, reducing the storage space of spare parts needed on site [5]

The advantages of the additively manufacturing process has resulted in a high interest from the industry. Examples of this might be such as Equinor [7] where the goal is to be able to reduce downtime

due to failure of production critical parts. They propose this can be performed by having a digital inventory and drones. In fact, a part could then be printed locally by a manufacturer, for then to be sent to the offshore facility with drones. Consequently, resulting in a "just-in-time" production of spare parts. Another example/motivation for additive manufacturing might be such as the reduction of weight in the aerospace industry [8]. The energy industry is also interested in the additive manufacturing of parts, due to such as fast prototyping, as the development of gas turbines involves trial and error. Thus, fast prototyping accelerates gas turbine development. Additionally, both the aerospace and energy sectors are commonly using complex parts, such as sophisticated air-cooling channels, which can easily be produced in the additive manufacturing process [9].

There is a large selection of metal AM technologies, which often include the melting of powder or wire feedstock using various energy or heat sources [10, 11]. The most accepted or alternatively most used methods for AM might be categorized as powder bed fusion (PBF) and direct energy deposition (DED). It is commonly accepted that the PBF has a high precision, whereas DED has a better production speed. Furthermore, it should be mentioned that the manufacturing/production parameters will significantly affect the resulting part [5]. This from the perspective that both methods iteratively add layer by layer by iteratively melting new material on the previously placed layer.

An issue with the AM technology, is the challenge of controlling the properties of the final product [12]. The AM process is commonly having issues such as pores, voids, surface roughness, loss of alloying elements, cracking, delamination, residual stresses, deformation etc. This due to the complex thermal history, resulting from laser speed, laser energy, scanning path strategy and powder/layer thickness etc. [5, 13]. However, bound metal composition (BMD) is a relatively new technology, promising a significant reduction in cost, while producing quality parts [14]. Furthermore, the technology does not iteratively melt or sinter layer by layer, thus, removing the perspective of the complex thermal histories/cycles.

Herein, the method of bound metal deposition is adapted to produce monotonic tensile test specimens. Specimens were designed and tested in accordance with ASTM E8/E8M for tension testing. Various printing orientations were used, to investigate the directional dependence on the mechanical properties. Furthermore, samples were prepared for inspection with an optical light microscope. Anisotropic behavior was found from the tension testing, for then to be correlated with defects found during inspection of the polished samples with an optical light microscope. Furthermore, the findings are discussed in light of mechanical properties and fatigue, for then to propose further research.

2. Bound metal deposition

The method adapted for printing is the method named Bound Metal Deposition by Markforged and Desktop Metal (DM). The manufacturing process can be described to have four steps, namely; (a) printing, (b) debinding, (c) sintering and (d) post processing. (a) firstly, powder-filled wire of polymer-wax binder is heated up and extruded layer by layer to develop the generated and sliced geometry. (b) Thereafter, the printed specimen is put in a washer to go through a debinding process to partly remove the binder. (c) After debinding has been performed, the specimen will be sintered to both remove the remaining binder, and to bind the metal particles together, resulting in a solid metal part. The sintering process is performed through placing the specimen in a furnace, with a slow uniform heat development and subsequent cooling in an inert gas. (d) The last step is post processing, this might be such as machining or polishing to achieve a better surface finish in regard to fatigue capacity, or alternatively hot isostatic pressing (HIP) to reduce pore structure, or alter the microstructure [14, 15].

It should be mentioned that the methodology of BMD is a fairly new technology. However, some advantages to the printing technique might be such as:

1. The BMD technology is expected to be roughly 60% less expensive than similarly sized PBF system [16].
2. There are fewer safety concerns with the BMD technology, with no need for a dedicated operator or powder management system [14]

3. As the sintering process is performed after the geometry of the part has finished printing, it is believed that the final product will have a better microstructure with low to none residual stresses in comparison to similar methods. Consequently, achieving favourable mechanical properties.

2.1 Printing scheme/strategy

The printing strategy of the machine is commonly to build a wall surrounding the geometry, which can be defined by the user between 2-8 wall layers. The wall layers are simply lines surrounding the geometry, developing the perimeter of the specimen. However, it should be noted that successive layers will be placed directly above the previous, in the same direction, unless the cross-sectional area is changing with height. Furthermore, the internal part of the specimen is the remaining cross-sectional are after the wall has been placed. The internal area is filled with layers, where the layers alternate between ±45º for each layer.

3. Experimental work

The material which was used during the experimental work was 17-4 PH stainless steel, which is a heat treatable precipitation hardening martensitic stainless steel. Commonly used in situations where corrosion resistance is required, such as aerospace, petroleum and chemical industries [6, 16].

As previously mentioned, the method for printing is by the BMD method, where the specimens were produced at the University of Stavanger by the use of a Markforged Metal X BMD printer. The printed specimens were tension tested to determine the mechanical properties as follows: Ultimate strength (UTS), yield tensile strength (YTS), Young's modulus (E) and elongation at break (%). Thereafter, the obtained results were compared to the documentation provided by Markforged for AM 17-4 PH stainless steel in the "as-sintered" condition. Furthermore, the printed specimens were inspected by the use of an optical light microscope, with the objective of determining the cause of the observed variation in mechanical properties.

3.1 Sample manufacturing

Specimens were designed in accordance with the ASTM E8/E8M subsize specimen, and can be seen in Figure 1 [17]. Thereafter, they were printed using a Markforged Metal X printer, which has a maximum build volume of 300x220x180mm, by the use of 17-4 PH stainless steel wire, supplied by Markforged. All the specimens were printed with 8 wall/perimeter layers, whereas the remaining internal section is printed with the alternating ±45º pattern. Subsequently, the specimens produced were washed, for then to be sintered to achieve the "as-sintered" condition. Herein, the step of post processing is skipped, other than removing the support structure.

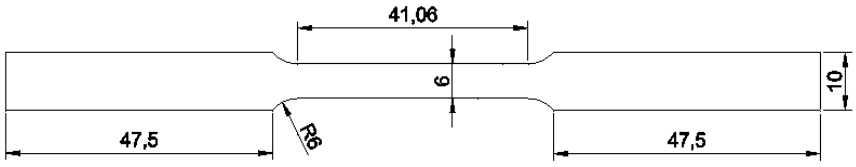

Figure 1. Specimen in accordance with ASTM E8/E8M, in mm.

A total of 9 specimens were manufactured, where three specimens were produced for three different printing directions. The first group consists of horizontally oriented specimens, which were called XY-flat. These specimens were built after 68 successive layers. The second group was rotated 90 degrees in relation to the x axis, consequently result in the need for a support structure while printing. These specimens were called XY-sided, and were built after 100 layers. The third group contained vertically printed specimens, which were called ZX. These specimens were built after 1175 layers. The build direction of the specimens XY-flat, XY-sided and ZX can be seen in Figure 2 a), b) and c) respectively.

For the optical light microscope, two samples were produced, one bar which was built in the vertical direction (V) with the dimensions 10x10x50 mm, and one built in the horizontal direction (H) with the

dimensions 50x10x10 mm as shown in Figure 2 d). This to be able to inspect for defects in regard to the printing orientation.

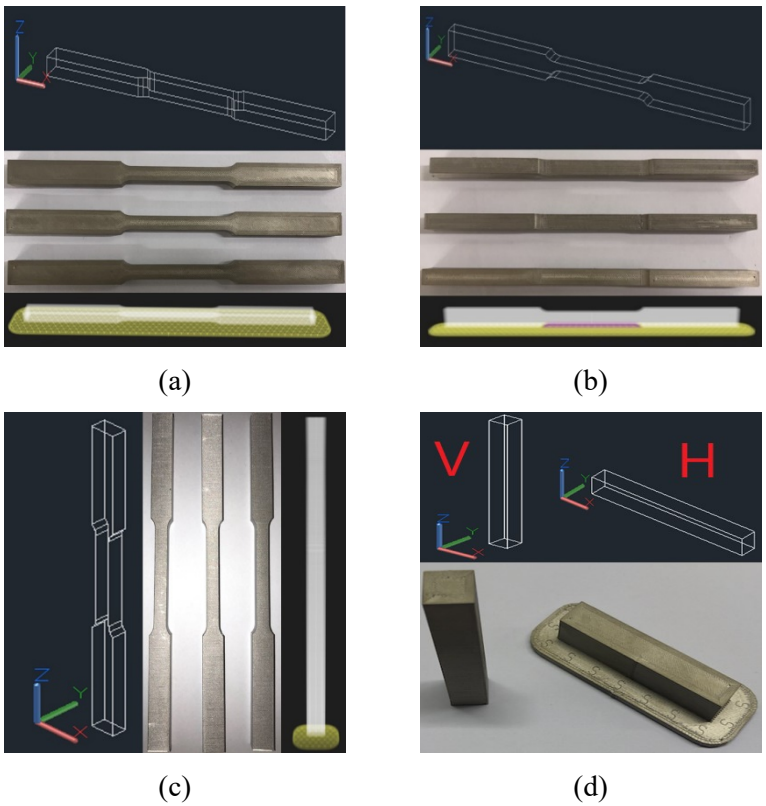

(a) (b)

(c) (d)

Figure 2. Printed specimens, (a) XY-flat, (b) XY-sided, (c) ZX, (d) vertical and horizontal print

3.2 Tension testing results

All the tension specimens were monotonically loaded until failure, in accordance with the standard ASTM E8/E8M. The resulting stress-strain curves for the specimens can be seen in Figure 4 and the fractured specimens can be observed in Figure 3. Furthermore, the resulting mechanical properties were tabulated, as can be seen in Table 1.

From the stress-strain curve presented in Figure 4, it can clearly be seen that most of the specimens (XY-sided and ZX) fail before any significant plasticity is achieved. Consequently, resulting in effectively a brittle failure, due to the choice of printing direction. In Figure 3, the various fractured specimens are presented. It can be seen that the XY-flat and ZX specimens commonly will fracture in the gauge length, whereas the XY-sided specimens will fail at the shoulder. This is believed to be due to defects being generated during the printing process in the shoulder for the XY-sided specimens. Furthermore, from the tabulated results, it can clearly be observed that the only specimens which have comparable mechanical properties to what is stated by Markforged, is the XY-flat specimens.

Figure 3. Fractured specimens

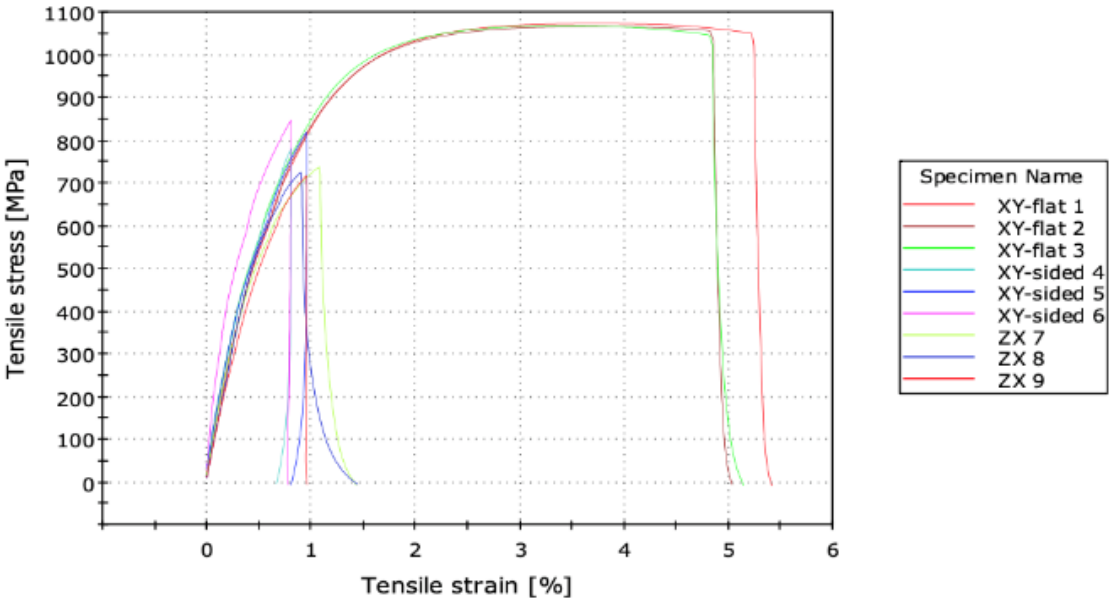

Figure 4. Stress-strain curves for the specimens

Table 1. Summary of mechanical properties

Specimen	0 2% Yield strength (MPa)	Ultimate tensile strength (MPa)	Young's modulus (GPa)	Elongation at break (%)
Markforged as-sintered [18]	800	1050	140	5
XY-flat 1	661,00	1072,00	136,74	5,24
XY-flat 2	764,30	1065,00	115,59	4,85
XY-flat 3	638,80	1067,00	161,53	4,84
XY-sided 4	699,80	780,80	135,54	0,81
XY-sided 5	637,60	817,50	145,63	0,96
XY-sided 6	613,30	846,70	286,87	0,80
ZX 7	579,40	737,70	139,73	1,09
ZX 8	656,60	725,50	128,68	0,91
ZX 9	610,10	717,20	123,83	0,95

3.3 Optical light microscope inspection

The specimens used for microscope inspection were the samples displayed in Figure 2 d). The specimens were cut using a Struers Discotom-5 machine. After cutting, the specimens were cleaned, rinsed and dried. The samples were prepared to be able to investigate both the top and side view of the vertical and horizontally printed part. The samples were iteratively polished, as follows:

1. 220 µm grit for 2 minutes.
2. Diamond suspension (9 µm) 3 minutes.
3. Diamond suspension (3 µm) 3 minutes
4. Chem OP-AA oxide polishing 2 minutes

The samples were cleaned between each of the aforementioned steps, by the use of an ultrasonic cleaner (Struers Lavamin machine) to remove any remaining particles from the previous step. The resulting images taken from the optical light microscope can be seen in Figure 6.

From the images presented, it can clearly be seen that the material exhibits a mesh of defects throughout the specimen. This mesh of defects also seems to be related to the printing scheme used by the machine. By observing the top view of the polished specimens (Figure 6 a) and c)), it can be seen that there are continuous lines, similar to the printing scheme/strategy previously mentioned. Figure 6 c) especially show how the walls or outer perimeter was developed with 8 layers, whereas the internal region has a 45º angle to the outer perimeter. It is also noted that each of these layers have a continuous defect/line between each of the printed perimeter or "walls".

Furthermore, by looking at the examples presented in Figure 7, where a representation is made in regard to how the walls are printed and how the internal filling is performed, a) and b) respectively, it can be seen that the area within the red squares have a similar shape to the defects found in Figure 6 b) and d). Consequently, strengthening the argument that the defects come due to the method of printing.

The defects which were found were estimated using the software Olympus stream essentials, where it was found that the shortest dimension of the triangular defects would commonly be on the range 22-33µm, whereas the longest dimension would commonly be on the range 39-86 µm. The square defect would commonly have a diagonal length on the range of 66-83 µm.

Additionally, the surface roughness of the "as-printed" specimens, due to the iterative layers during the printing process can be observed in Figure 5. The measured distance from top to bottom was on the range 43-54µm. However, it should be noted that the surface condition mentioned here, is only in regard to the iterative layers placed, and the surface will not be as rough along the grooves of the roughness/layers presented here. As in the direction into or out of the picture.

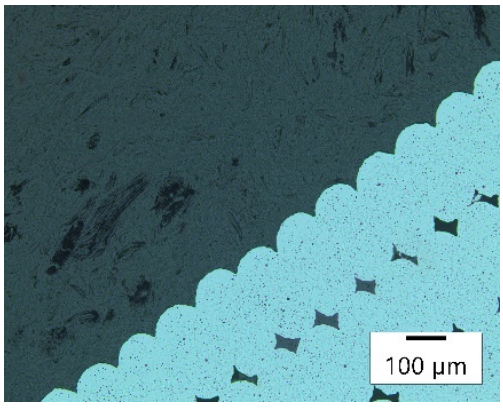

Figure 5. Surface condition

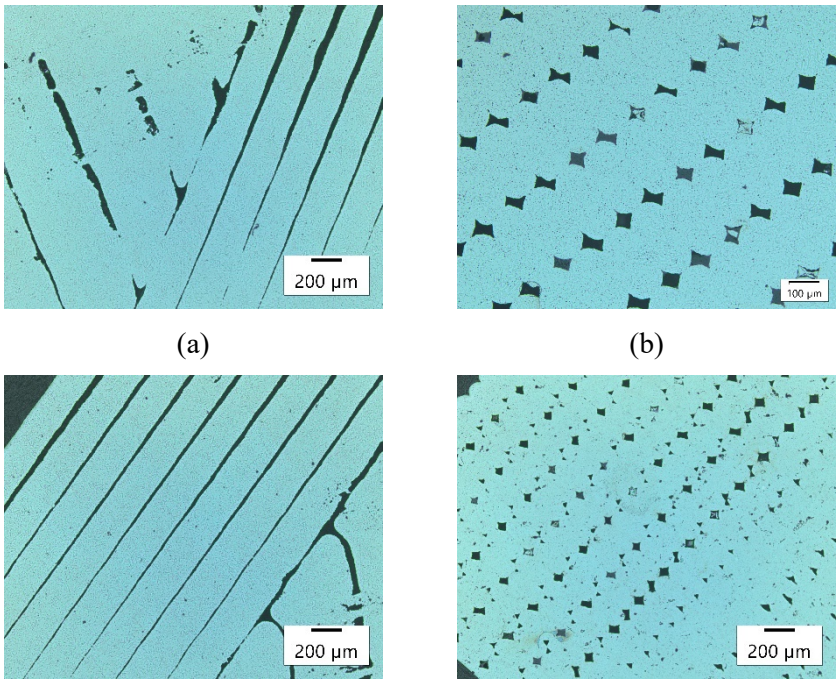

Figure 6. Images taken from optical light microscope, (a) top view vertical printed, (b) side view vertical printed, (c) top view of horizontal print, (d) side view of horizontal print

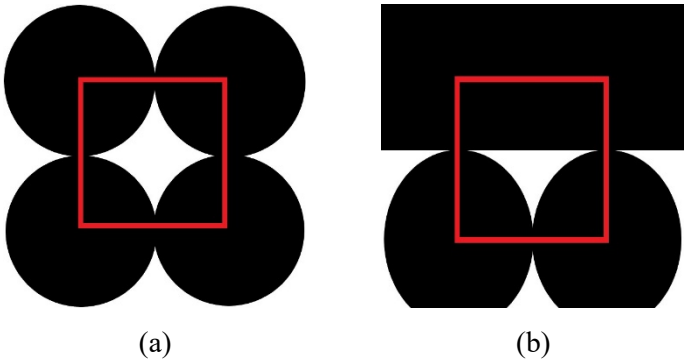

Figure 7. Representations of defects found in the printed material, (a) square defect, (b) triangle defect

4. Discussion

4.1 Mechanical properties and defects

The specimens manufactured in the horizontal direction without any support (XY-flat) specimens, exhibited comparable ultimate tensile strength and elongation at break as listed by Markforged for the as-sintered condition. In contrast to the XY-flat printed specimens, both the XY-sided and ZX printed specimens exhibited worse mechanical properties than listed by Markforged for the as-sintered condition. Furthermore, the specimens XY-sided commonly fractured outside of the gauge length. This possibly due to a defect produced during the printing process.

The results obtained by tension testing the specimens clearly show that the build orientation of the specimens affects the resulting mechanical properties of the metal parts. Furthermore, during the light microscope inspection of the polished parts, it was found that there is a clear pattern of directional

defects which are directly correlated to the printing orientation. Consequently, resulting in the anisotropic behaviour observed in the experimental work.

Through the use of the images taken and presented in Figure 6, it can be seen that two defects commonly occur from the side view. One exhibits a shape similar to a diamond/square, whereas the other exhibits more a shape of a triangle, as is depicted in Figure 7. In fact, the defects within each specimen will be as follows in the reduced section:

1. Horizontally built flat (XY-flat): The outer wall will exhibit longitudinal defects as depicted in Figure 7 a), however, as the stress will act parallel to the length direction of the defect, minimal reduction of capacity is expected. The internally filled area will exhibit defects as presented in Figure 7 b), with a 45-degree angle to the applied loading direction. Furthermore, the grooves of the roughness presented in Figure 5 will also be parallel to the loading direction, consequently expecting it not to have a significant effect.
2. Horizontally built rotated (XY-sided): The outer wall, in the commonly failure region, will exhibit defects similar to the ones presented in Figure 7 a). However, at the shoulder of the specimen, the flaws will be perpendicular to the loading direction, potentially describing the cause and location of failure. The surface at the shoulder section will also be rough, similar to the roughness shown in Figure 5, in the direction perpendicular to the applied stress. Furthermore, the interior will have similar flaws as the interior in the previously explained specimen, however rotated by 90 degrees. In the gauge length, the specimen will again have a similar defect mesh as presented for the previous specimen. This explains the reason why it failed at the shoulder.
3. Vertically built (ZX): The outer wall will exhibit flaws similar to Figure 7 a), throughout the entire specimen, which will also be perpendicular to the loading direction. In addition, the surface roughness of the section will be as presented in Figure 5, where the applied loading will act perpendicular to the roughness/grooves. Furthermore, the internal section of the specimen will have a mesh of defects as presented in Figure 7 b), where the applied loading will act perpendicular to the longest direction of the defects, which was on the range 39-86μm.

The mechanical properties and light microscopy inspection and the discussion herein coincide well. This from the perspective that the mechanical properties are easily explained by the defects observed within the material. From the defects observed, the ultimate tensile strength from best to worst should be 1. XY-flat, 2. XY-sided, 3. ZX, which is confirmed in Table 1.

4.2 Fatigue considerations

Herein, no fatigue tests were performed in regard to the BMD printing method. However, a general comment in regard to potential fatigue capacity should be made, considering some of the main industries motivating for additive manufacturing are such as automotive, aerospace, energy oil and gas, mentioned in the introduction. This from the perspective that automotive, aerospace and energy oil and gas industries all commonly have to consider dynamic loading.

From the tensile testing, it was clearly noted that the material exhibited anisotropic mechanical properties. Furthermore, during the inspection of the material with light microscopy, it was found that a mesh of defects, similar to cracks, were present. Consequently, resulting in that the following can be expected during fatigue loading:

1. The fatigue capacity will also be anisotropic.
2. The material/specimens might have a reasonable fatigue capacity for the specimens printed in the XY-flat orientation, however, both the XY-sided and ZX specimens are expected to have a very poor fatigue capacity. This from the crack's orientation to the applied cyclic loading.

4.3 Suggestions for further research

As previously mentioned, the printed specimens exhibited a fine mesh of defects, depending on the printing orientation of the specimen. Furthermore, the surface finish of the as-printed specimens was observed to be poor (rough surface). Therefore, it is believed that a post processing strategy might significantly improve the mechanical properties of the material. This might be such as:

1. Hot isostatic pressing (HIP) to reduce the size of the defects present in the specimen.
2. Machining the surface to achieve a smooth surface.

5. Conclusions

Herein, the method of BMD metal printing was assessed, in regards to printing direction, and defects present within the final product. Main activities and findings are presented as follows:

1. Specimens were manufactured by the BMD method with three different printing orientations, tension tested in accordance with ASTM E8/E8M and compared with the mechanical properties presented by Markforged.
2. Anisotropic behaviour in regard to the printing orientation was found.
3. Samples were prepared and inspected with the use of an optical light microscope, where a clear mesh of defects similar to cracks were noticed, and an estimated size was presented.
4. The mesh of defects was discussed and related to the mechanical properties.
5. Application of components printed by the BMD method was discussed in light of dynamic loading (fatigue) on the basis of the mechanical properties and defects found.
6. Suggestions for further research was proposed, as in the possibility of post processing to improve mechanical properties/behaviour.

Acknowledgement

The authors are grateful for the support provided by Jørgen Grønsund, Jan-Tore Jakobsen, Johan A. Thorkaas and Mats Ingdal during the experimental work.

References

[1] ASTM 2021 *Additive Manufacturing Overview*. [Online] [cited 09.09.2021]; Available from: https://www.astm.org/industry/additive-manufacturing-overview.html.
[2] Milewski J 2017Additive Manufacturing of Metals: From Fundamental Technology to Rocket Nozzles, Medical Implants, and Custom Jewelry. Additive Manufacturing of Metals,.
[3] Zadi-Maad A, Rohib R and Irawan A 2018 Additive manufacturing for steels: a review. *IOP Conf Series*: *Mater Sci Eng* **285**, 012028.
[4] Ngo T D, Kashani A, Imbalzano G, Nguyen K T Q and Hui D 2018 Additive manufacturing (3D printing): A review of materials, methods, applications and challenges. *Compos Part B*: Eng,. **143**, 172-96.
[5] DebRoy T, Wei H L, Zuback J S, Mukherjee T, Elmer J W, Milewski J O, et al., 2018 Additive manufacturing of metallic components – Process, structure and properties. *Progress Mater Sci* **92**, 112-24.
[6] Molaei R and Fatemi A 2019 Crack paths in additive manufactured metallic materials subjected to multiaxial cyclic loads including surface roughness, HIP, and notch effects. *Int J Fatigue* **124**, 558-70.
[7] Equinor. From designer's dream to production reality: Spare parts on the fly. [Online] 2021; Available from: https://www.equinor.com/en/magazine/fieldmade-3d-printing-spare-parts.html.
[8] Blakey-Milner B, Gradl P, Snedden G, Brooks M, Pitot J, Lopez E, et al., 2021 Metal additive manufacturing in aerospace: A review. *Mater Des.* **209**, 110008.
[9] Appleyard D 2015 Powering up on powder technology. Metal Powder Report,. **70**(6), 285-89.
[10] Herzog D, Seyda V, Wycisk E and Emmelmann C 2016 Additive manufacturing of metals. *Acta Materialia*. **117**, 371-392.
[11] Nezhadfar P D, Burford E, Anderson-Wedge K, Zhang B, Shao S, Daniewicz S R, et al., 2019 Fatigue crack growth behavior of additively manufactured 17-4 PH stainless steel: Effects of build orientation and microstructure. *Int J Fatigue* **123**, 168-79.

[12] Afkhami S, Dabiri M, Alavi S H, Björk T and Salminen A 2019 Fatigue characteristics of steels manufactured by selective laser melting. *Int J Fatigue* **122,** 72-83.
[13] Wang Z, Wu W, Qian G, Sun L, Li X and Correia J A F O 2019 In-situ SEM investigation on fatigue behaviors of additive manufactured Al-Si10-Mg alloy at elevated temperature. Engineering Fracture Mechanics,. **214**, 149-63.
[14] Markforged. Metal X System. [Online] [cited 2021 13.09.2021]; Available from: https://markforged.com/3d-printers/metal-x.
[15] Desktop-metal. Deep Dive: Bound Metal Deposition (BMD). [cited 2021 13.09.2021]; Available from: https://www.desktopmetal.com/resources/deep-dive-bmd.
[16] Watson, A., J. Belding, and B.D. Ellis, Characterization of 17-4 PH Processed via Bound Metal Deposition (BMD). 2020. Cham: Springer International Publishing.
[17] ASTM-International, ASTM E8 / E8M-21: Standard Test Methods for Tension Testing of Metallic Materials. 2021.
[18] Markforged. 17-4 PH Stainless Steel - Datasheet. [Online] 2021 15.09.2021]; Available from: https://markforged.com/materials/metals/17-4-ph-stainless-steel / https://static.markforged.com/downloads/17-4-ph-stainless-steel.pdf.